# Morphology and Thermal and Dielectric Behavior of Cycloaliphatic Epoxy/Trimethacrylate Interpenetrating Polymer Networks for Vacuum-Pressure-Impregnation Electrical Insulation

**Jingkuan Duan,[1] Chonung Kim,[1,2] Zheng Yun,[1] Pingkai Jiang[1]**

[1]*Shanghai Key Laboratory of Electrical Insulation and Thermal Aging, Shanghai Jiaotong University, Shanghai 200240, People's Republic of China*
[2]*Department of Electrical Engineering, Kim Chaek University of Technology, Pyongyang, D. P. R. of Korea*

Received 17 March 2008; accepted 2 June 2008
DOI 10.1002/app.28835
Published online 8 September 2008 in Wiley InterScience (www.interscience.wiley.com).

**ABSTRACT:** Vacuum pressure impregnation has been known as the most advanced impregnation technology that has ever been developed for large and medium high-voltage electric machines and apparatuses. We developed one new type of vacuum-pressure-impregnation resin with excellent properties by means of a novel approach based on *in situ* sequential interpenetrating polymer networks resulting from the curing of trimethacrylate monomer [trimethylol-1,1,1-propane trimethacrylate (TMPTMA)] and cycloaliphatic epoxy resin (CER). In this study, the influence of the concentrations of the components and their microstructures on their thermal and dielectric behaviors were investigated for the cured CER/TMPTMA systems via atomic force microscopy, dynamic mechanical analysis, thermogravimetric analysis, and dielectric analysis. The investigation results show that the addition of TMPTMA to the CER–anhydride system resulted in the formation of a uniform and compact microstructure in the cured epoxy system. This led the cured CER/TMPTMA systems to show much higher moduli in comparison with the pure CER–anhydride system. The thermogravimetric analysis results show that there existed a decreasing tendency in the maximum thermal decomposition rates of the cured CER/TMPTMA systems, which implies that the thermal stability properties improved to some extent. The dielectric analysis results show that the cured CER/TMPTMA systems displayed quite different dielectric behaviors in the wide frequency range 0.01 Hz–1 MHz and in the wide temperature range 27–250°C compared with the cured CER–anhydride system. © 2008 Wiley Periodicals, Inc. J Appl Polym Sci 110: 3096–3106, 2008

**Key words:** curing of polymers; interpenetrating polymer networks (IPN); networks

## INTRODUCTION

The impregnation of high-voltage (HV) electrical apparatuses, for example, large HV generators, motors, and power transformers, has been known as a most necessary measure, not only to provide the required electrical insulation performance but also to prevent the mechanical vibration of the electrical insulation structure caused by the electromagnetic field and to obtain high thermal conductivity in the insulation structure to enable the increase of the current density in the coils without exposure of the organic electrical insulating materials to excessively high temperatures.[1–4] Particularly, vacuum pressure impregnation (VPI), which exhibits various merits including the improvement of insulation performance, stabilization of quality, shortening of manufacturing period, and mitigation of maintenance load, is the most advanced impregnation technology that has ever been developed for large and medium HV electric machines and apparatuses.

Epoxy and its composites have been known as suitable synthetic insulating materials for VPI technology of HV machine insulation and have been widely used as one of the main insulating materials in both electric power and electronic industries because of their superior electrical, mechanical, and thermal properties, economical cost, and convenient processability. With the development of the electrical industry, the requirements of the properties of VPI resins has become higher and higher, and much effort has been devoted to the modification of the mechanical, thermal, and electrical properties of epoxy resin.[5–15] One new type of VPI resin, which contains *in situ* sequential interpenetrating polymer networks (sIPNs) resulting from the curing of cycloaliphatic epoxy resin (CER) and trimethacrylate

*Correspondence to:* P. Jiang (pkjiang@sjtu.edu.cn).
Contract grant sponsor: Shanghai Committee of Science Technology through the Funds for Major Research Projects of Shanghai City; contract grant number: 05dz22303.

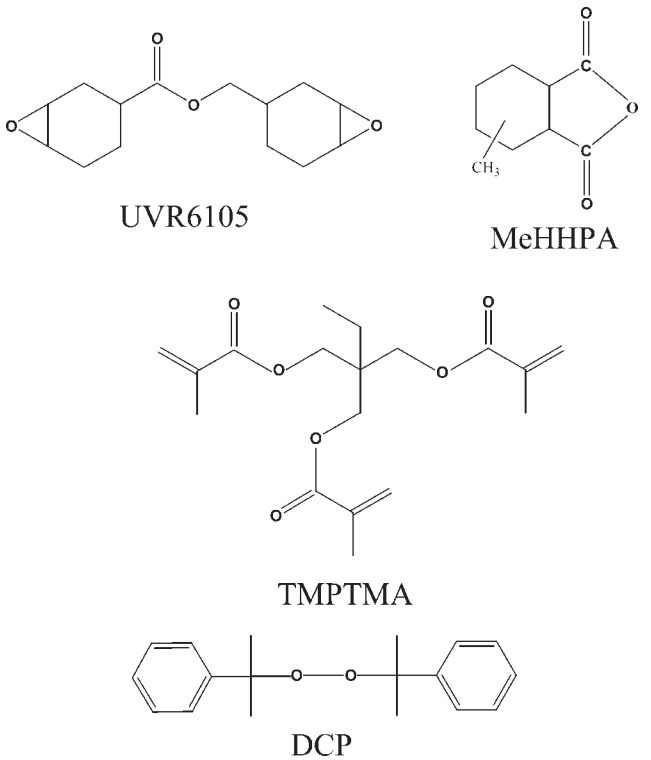


**Figure 1** Chemical structures of the raw materials.

monomer [trimethylol-1,1,1-propane trimethacrylate (TMPTMA)], with more excellent properties than conventional VPI resins was developed in our previous study.[16]

The macroscopic properties of polymeric materials are strongly dependent on their microstructures, which can lead the crosslinking structure of an epoxy resin to influence its physical, chemical, thermal, electrical, and mechanical properties. This points us to the fact that the measurement of the properties of cured epoxides allows one to understand and characterize some interesting phenomena taking place during the epoxy curing procedure, for example, the molecular structures, crosslinking degree, network formation, and ionic mobility.

During the past decade, a number of diagnostic techniques have been developed to evaluate the crosslinking degree of epoxy resins, including infrared spectroscopy,[14] differential scanning calorimetry,[15] and viscosity.[17] All of these techniques not only require well-equipped laboratory conditions and the destruction of the samples used but also are usually complex and costly to implement. Dielectric response analysis has been widely used in electrical insulating engineering for different purposes, such as the qualification of insulating materials and systems or for the *in situ* diagnosis of HV apparatuses in a nondestructive manner.[18–23]

The objective of this study was to further elucidate the relationships between the microstructures of the resulting interpenetrating polymer networks (IPNs) composed of CER–anhydride and TMPTMA monomers and their macroscopic properties, including their thermal and dielectric properties, on the basis of the previous studies.[16]

In this study, atomic force microscopy (AFM) measurement was adopted to evaluate the microstructures of the resulting IPNs. Dynamic mechanical analysis (DMA) was used to study the elastic modulus, which was used to calculate the theoretical molecular weight between crosslink points of the resulting IPNs. Thermogravimetric analysis (TGA) was applied to estimate the thermal behaviors of the resulting IPNs, and dielectric analysis (DEA) was used to explore the dielectric behaviors of the resulting IPNs.

## EXPERIMENTAL

### Materials

3,4-Epoxycyclohexylmethyl 3′,4′-epoxycyclohexane carboxylate (marketed under the trade designation UVR6105) was purchased from Dow Chemical Co. (Midland, MI). The curing agent was methyl tetrahydrophthalic anhydride (MeHHPA; marketed under the trade designation LHY-807), which was purchased from Shanghai Li Yi Science and Technology Development Co., Ltd. (Shanghai, China). The latent accelerator was neodymium(III) acetylacetonate hydrate [Nd(III)AcAc; marketed under the trade designation FLQ-1], which was purchased from Qinyang Tianyi Chemical Co., Ltd. (Qinyang City, Henan Province, China). The modifier agent was TMPTMA, a trifunctional acrylate (marketed under the trade designation TMPTMA), which was obtained from Jinshi Tech-Development Co., Ltd. (Nanjing City, Jiangsu Province, China). The initiator, dicumyl peroxide (DCP), was purchased from Aldrich Chemical Company (Milwaukee, WI). The chemical structures of the epoxy resin and the curing and modifier agents are shown in Figure 1.

### Sample preparation

The epoxy resin and curing and modifier agents underwent a sole extended hold for degassing *in vacuo* (ca. −0.15 MPa) at 100°C for about 30 min until the bubbles disappeared, and the latent accelerator and initiator were used without purification.

Epoxy resin [100 parts by weight (pbw)] and latent accelerator (0.5 pbw) were weighed and mixed vigorously at 160°C for about 10 min until the latent accelerator was dissolved completely in the epoxy resin. Then, the blends of epoxy resin and accelerator were rapidly cooled to the ambient temperature; this was followed by the addition of 95 pbw curing

**TABLE I**
**Formulations of the Experimental Systems**

| Sample | UVR6105 (pbw) | LHY-807 (pbw) | Nd(III)AcAc (pbw) | TMPTMA (pbw) | DCP (pbw) |
|---|---|---|---|---|---|
| 1 | 100 | 95 | 0.5 | 0 | 0 |
| 2 | 100 | 95 | 0.5 | 20 | 0.02 |
| 3 | 100 | 95 | 0.5 | 40 | 0.04 |
| 4 | 100 | 95 | 0.5 | 60 | 0.06 |

agent and suitable amounts of the initiator and modifier agent according to the formulation given in Table I and mixing for about 10 min. After the liquid mixture underwent an extended hold for degassing *in vacuo* (ca. −0.15 MPa) at ambient temperature for about 30 min, rectangular bar samples [(1 × 6 × 20 $mm^3$ (thickness × width × length)] and circular plate samples (diameter = 110 mm, thickness = 1 mm) for measurement of the dynamic mechanical behavior and electric properties, respectively, were cured in open stainless steel molds for 4 h at 135°C and then postcured at 165°C for 14 h.

### Analytical measurements

#### Density measurement

The density measurement of the cured IPN specimen was carried out in accordance with the testing method B pycnometer method in GB1033-1986 (the test method for the density and relative density of plastics). The calculation of density was performed with the following equation:

$$\rho_t = \frac{m\rho_x}{m_1 - m_2}$$

where $\rho_t$ is the density of the cured sample ($g/cm^3$), $m$ is the weight of the cured sample (g), $m_1$ is the weight of water in the pycnometer, $m_2$ is the total weight of water and the cured sample (g), and $\rho_x$ is the density of water at 23°C (0.9976 $g/cm^3$).

#### AFM

The morphological observation of the fractured surface of the samples was conducted on a Nanoscope IIIa scanning probe microscope (Digital Instruments, Santa Barbara, CA) in tapping mode. A tip fabricated from silicon (length = 45 μm, resonant frequency ≈ 500 kHz) was applied for scanning, and the scanning rate was 2.0 Hz.

#### TGA

TGA measurement was carried out with 5–10 mg of the cured CER/TMPTMA systems at a heating of 10°C/min under a nitrogen atmosphere with a TGA analyzer (Cahn TG Systems 41 thermogravimetric analyzer, ThermoFisher Scientific, Waltham, MA). The samples were subjected to TGA in high-purity nitrogen under a constant flow rate of 10 mL/min. The thermal decomposition of each sample occurred in the programmed temperature range 20–800°C. The continuous records of weight loss and temperature were determined and analyzed to determine the following TGA indices: thermal degradation temperature and thermal degradation rate (weight loss %/°C).

#### DMA

DMA spectra were taken with rectangular bar specimens in the flexural model at 1 Hz with an Eploxor 150N device (Gabo, Ahlden, Germany). The cyclic (sinusoidal) loading components were set as 1 N. DMTA spectra, namely, the elastic modulus as a function of temperature, were measured in the temperature range 30–250°C.

#### DEA

Dielectric responses were measured with a Concept 40 band frequency impedance analyzer (Novocontrol Company, Hundsangen, Germany) in the frequency range $10^{-2}$–$10^6$ Hz and at different temperatures ranging from room temperature to 250°C.

The direct-current resistivity values of the cured CER/TMPTMA systems were measured with a ZC36 high-insulation resistance meter (Shanghai Precision and Scientific Instrument Co., Ltd., Shanghai, China) at different temperatures. In this study, the measurement began 30 min after the temperature inside the oven reached a selected value. The diameter of the measuring electrode was 50 mm, and the direct-current voltage applied to the sample was 500 V.

## RESULTS AND DISCUSSION

### Morphologies

Because of the nature of the raw materials chosen in this study, there could be two kinds of independent curing reactions during the formation of the IPNs composed of CER and TMPTMA: the thermal polyaddition of CER and the free-radical polymerization of TMPTMA initiated by initiator. These two curing reactions expected to exist in the CER–anhydride/

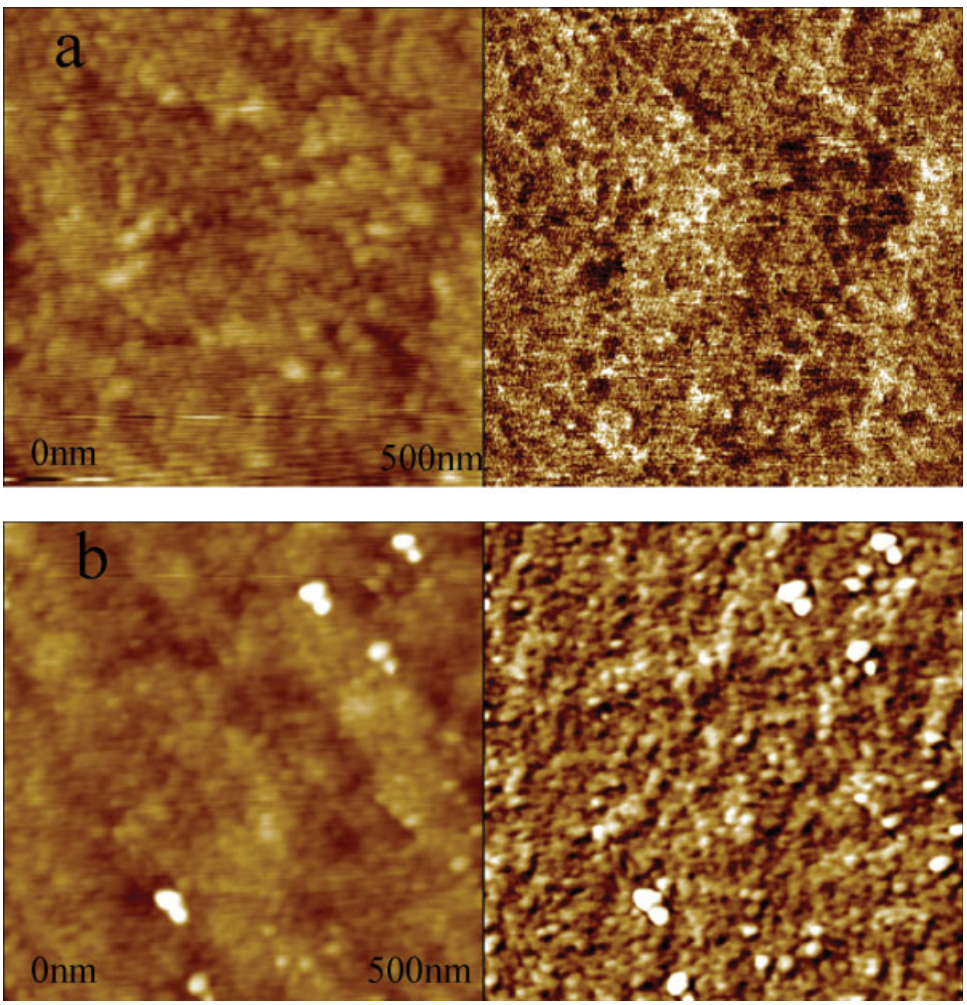


**Figure 2** AFM images (topography on the left and phase contrast on the right) of (a) the pure CER–anhydride system and (b) the CER/TMPTMA system (100/20). [Color figure can be viewed in the online issue, which is available at www.interscience.wiley.com.]

TMPTMA systems could display sequential reactions, which would result in the sIPNs. In our previous study, the formation of IPNs in these thermosetting systems was confirmed and characterized by means of optical measurements.[16]

To further determine the influence of the sequential reaction mechanisms of the cured CER–anhydride/TMPTMA systems on the microstructures of the resulting IPNs, the fractured surface sections of the cured thermosetting specimens were subjected to morphological observations with AFM. Shown in Figure 2 are the AFM images of the CER–anhydride system and a representative IPN. The left and right images are the topography and phase contrast images, respectively. As shown in the topography images, all of the thermosetting specimens exhibited nodular structures, which were also found by Dusek et al.[24] The nodular structure was a consequence of the network buildup through the formation of microgels and their growth into clusters. Moreover, it was clear that the dimensions of the nodular particles existing in the cured IPNs were lower and more homogeneous than those existing in the pure CER–anhydride system. This may have been closely related to the two sequential curing reactions in the CER/TMPTMA systems.

The phase images showed that the cured CER/TMPTMA system possessed a more homogeneous and complete microstructure than the pure CER–anhydride system, which may have been due to the IPN formation between the CER–anhydride and TMPTMA, which revealed that the crosslinking density of the resulting IPNs was higher than that of the pure CER–anhydride system.

### Modulus and molecular weight measurements

To further validate the previous results obtained from AFM measurement, DMA was carried out. Figure 3 gives the elastic modulus of the cured

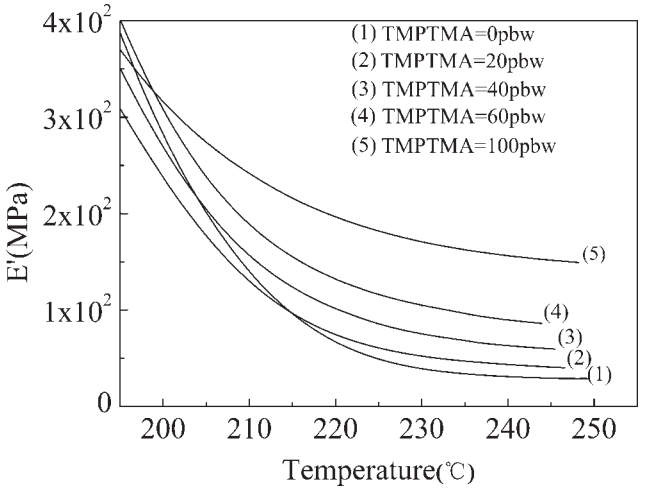


**Figure 3** Temperature dependence of the elastic modulus ($E'$) for CER/TMPTMA systems with different concentrations of TMPTMA.

CER/TMPTMA systems with different concentrations of TMPTMA as a function of temperature.

It is well known that the dynamic mechanical properties of thermosetting resins depend critically on the efficiency of the polymerization processes (the curing reactions) and are greatly influenced by their crosslinking degrees, especially above the glass-transition temperature.[25,26] As shown in Figure 3, the sequential IPNs showed a significant increase in the rubbery plateau modulus (as defined in ref. 27) compared to the neat epoxy resin and also displayed a dependence on the TMPTMA concentration and the temperature.

The density of a crosslinking network can be characterized in terms of the average molecular mass between crosslinks, which can be calculated from the dynamical mechanical storage moduli with an assumption of the validity of rubber elasticity theory. According to rubber elasticity theory, the value of the rubbery plateau modulus is proportional to the crosslinking density or inversely proportional to the average molecular mass between crosslinks, which can be expressed as a function of the rubbery plateau modulus with the following relationship:[28]

$$M_c = 3q\frac{\rho RT_R}{E_R} \quad (1)$$

where $M_c$ is the average molecular mass between crosslinks, $q$ is the front factor (the value of $q$ is close to unity), $E_R$ is the rubbery plateau modulus (MPa), $\rho$ is the density of the crosslinked network (g/cm$^3$), $R$ is the universal gas constant (8.32441 J/mol K), and $T_R$ is the plateau onset temperature (K). In eq. (1), it is assumed that the network is ideal and all of the chains are elastically effective. A higher value of the average molecular mass between crosslinks corresponds to a less crosslinked network.

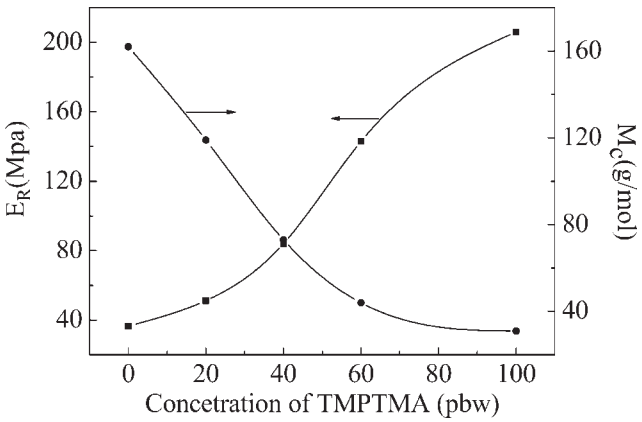


**Figure 4** Dependence of the elastic modulus ($E_R$) and the molecular weight between crosslinking points ($M_c$) for CER/TMPTMA systems on the TMPTMA concentration.

The results calculated with eq. (1) and the storage modulus values in the rubbery region obtained from DMA measurement are given in Figure 4. As shown in the calculation and measurement results, for the cured CER/TMPTMA systems, the average molecular mass between crosslinks tended to decrease gradually with increasing amount of TMPTMA, which implied that the total crosslinking density of the sequential IPNs, including chemical crosslinking (chemical bonds) and physical crosslinking (intermolecular tangles), was higher than that of the neat epoxy–anhydride system. At the same time, a distinct decreasing tendency was also observed in the rubbery plateau modulus with increasing TMPTMA concentration, which implied that the sequential IPNs possessed the higher stiffness. These

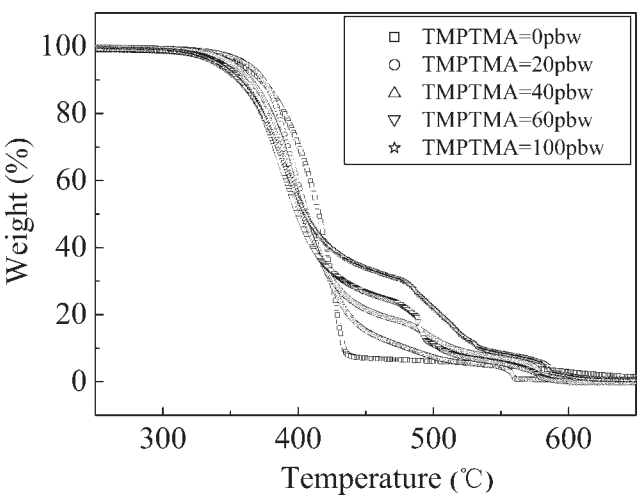


**Figure 5** TGA results for CER/TMPTMA systems with different concentrations of TMPTMA as a function of temperature.

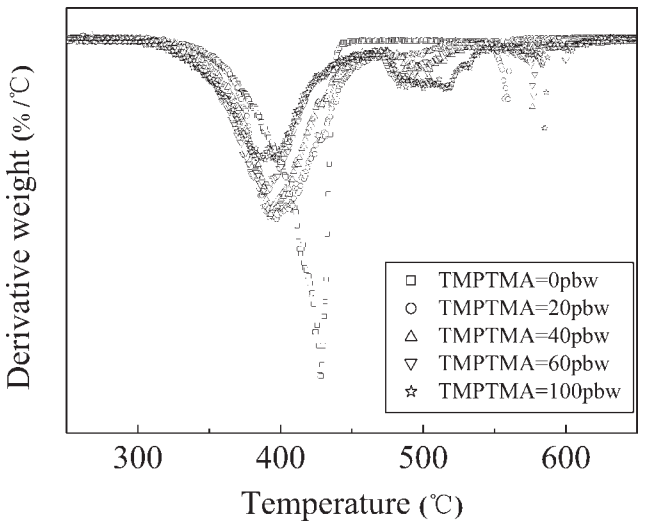


**Figure 6** DTA results for CER/TMPTMA systems with different concentrations of TMPTMA as a function of temperature.

results were also strongly supported by AFM measurements.

### Thermal behavior measurement

The weight loss of a material as function of time or temperature is commonly determined with TGA, and it is an irreversible process because of the thermal degradation. The TGA curves of the pure CER–anhydride system and the cured CER/TMPTMA systems with different concentrations of TMPTMA are shown in Figure 5. For the pure CER–anhydride system, the initial degradation temperature of the material occurred at about 350°C, which was similar to that of the cured sample containing 20 pbw TMPTMA but slightly lower than that of the cured sample in which the TMPTMA concentration was above 40 pbw. However, it was not a simply monotonic relationship between the initial weight loss temperature and the concentration of TMPTMA. When the concentration of TMPTMA was above 60 pbw, the initial weight loss temperature hardly decreased. Interestingly, there existed a second thermal decomposition reaction between 450 and 600°C, which could be assigned to the decomposition reaction of the TMPTMA component, whereas the first thermal decomposition reaction could be attributed to the decomposition reaction of the CER–anhydride component. This could be also used to prove the existence of IPNs in the cured CER/TMPTMA systems and was in good agreement with the results from our previous study.[16]

The dynamic thermal analysis (DTA) results of the cured CER/TMPTMA systems with different concentrations of TMPTMA as a function of temperature are depicted in Figure 6. The maximum weight loss rate of the cured CER–anhydride system occurred at 430°C, whereas for the cured CER/TMPTMA systems, it was observed between 380 and 390°C, which revealed that the addition of TMPTMA to the CER–anhydride system led to an increase in the maximum weight loss rate temperature. Although a depressed tendency in the initial weight loss temperature and maximum weight loss rate temperature were observed as the concentration of TMPTMA increased in the cured CER/TMPTMA systems, it is worth noting that the maximum weight loss rates of the IPNs composed of CER and TMPTMA decreased distinctly compared with that of the pure CER–anhydride system. In addition, the maximum weight loss rates of the IPNs gradually decreased as the concentration of TMPTMA in the IPNs increased. We deduced that the incorporation of TMPTMA monomers into the crosslinking networks may have acted as a hindrance for the formation of the crosslinking structures of the CER–anhydride system during the formation of IPNs but that it could slow the thermal decomposition rate of the resulting IPNs; this implies that the presence of the crosslinking network of the TMPTMA monomer could enhance the thermal stability of the resulting IPNs to some extent.

### Dielectric loss factor (tan δ) measurement

Figures 7 and 8 show the frequency dependences of tan δ for the cured epoxides with different concentrations of TMPTMA in the comparatively wide frequency range $10^{-2}$–$10^{6}$ Hz.

As shown in Figures 7 and 8(a), significant tan δ behaviors of the cured epoxides with different concentrations of TMPTMA were observed in the extra-low-frequency range below 0.1 Hz, where the tan δ values of the cured epoxides with and without TMPTMA tended to sharply decrease with increasing

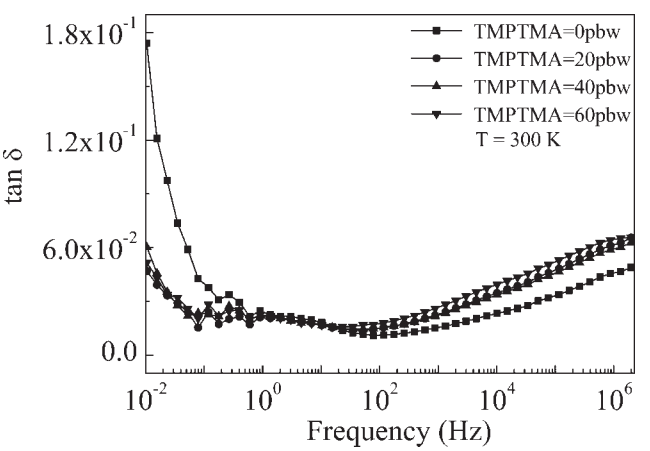


**Figure 7** Frequency dependences of tan δ for cured epoxides with different contents of TMPTMA.

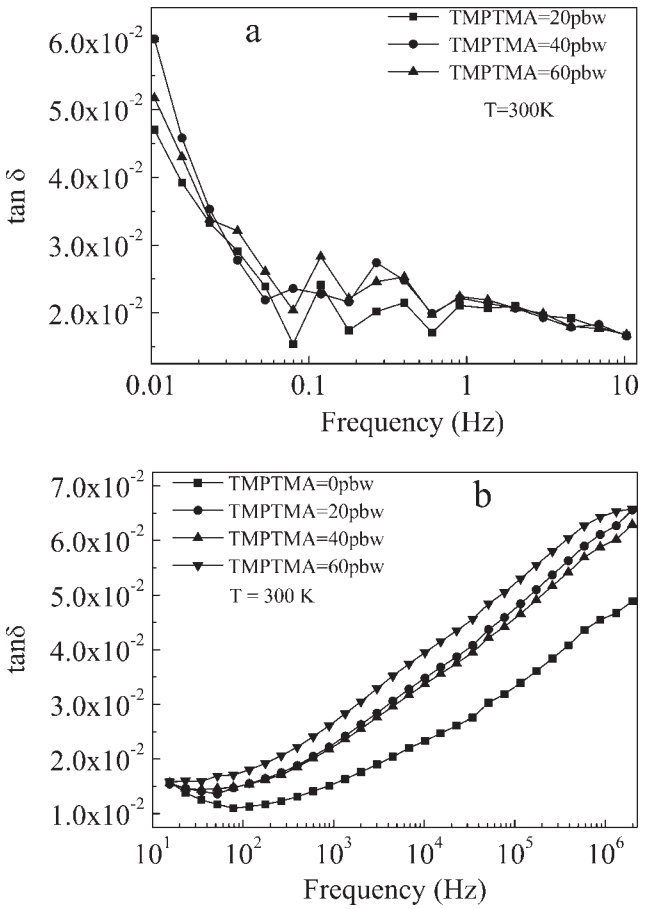


**Figure 8** Tan δ behaviors of cured epoxides with different concentrations of TMPTMA in (a) the extra-low frequency range and (b) the high frequency range.

frequency. The tan δ value in the extra-low-frequency range was much higher in the cured neat epoxide sample than in the cured CER/TMPTMA specimens, whereas few significant differences were found between the tan δ values of the cured epoxides with different TMPTMA concentrations.

The theory of the dielectrics[23] could be effectively used to interpret the tan δ behaviors of these cured thermosetting systems in the extra-low-frequency range: the dielectric loss caused by the alternating-current electric field could be attributed to both the conduction loss due to motions of free ions and to the relaxational loss due to the motion of electric dipoles:

$$\tan\delta = \frac{\gamma + \varepsilon_0(\varepsilon_s - \varepsilon_\infty)\dfrac{\omega^2\tau}{1+\omega^2\tau^2}}{\omega\varepsilon_0\left[\varepsilon_\infty + \dfrac{\varepsilon_s - \varepsilon_\infty}{1+\omega^2\tau^2}\right]} \quad (2)$$

where $\varepsilon_0$ is the dielectric constant ($8.85 \times 10^{-12}$ F/m); $\varepsilon_\infty$ and $\varepsilon_s$ are the dielectric permittivities when the frequencies of the applied electric field is infinitely large and nearly the same as zero, respectively; $\gamma$ is the ionic conductivity; $\omega$ is the angular frequency of the applied voltage; and $\tau$ is the relaxation time of the dipole polarization.

When a dielectric is placed in alternating-current electric field with a frequency below 0.1 Hz, the frequency is so low (nearly the same as direct-current electric field) that dipoles inside the dielectric move quite slowly and can be extremely thought to be "frozen" in the state of orientation toward the applied electric field, which leads to the conclusion that the dipole relaxed polarization can be nearly neglected and hardly contributes to the dielectric loss in the extra-low-frequency range. Moreover, it is well known that the lower the frequency of the applied electric field is, the larger the ionic current flowing through a dielectric is. Because $\omega$ is nearly equal to zero in the extra-low-frequency range, eq. (2) can be rewritten as

$$\tan\delta \approx \frac{\gamma}{\omega\varepsilon_0\varepsilon_\infty} \quad (3)$$

It is obvious from eq. (3) that the lower the frequency is and the higher the ionic conductivity is, the larger tan δ is.

For most commercial applications with epoxy resins, it is necessary to add a kind of accelerator, usually in the form of a base, acid, or organometallic compound, to the formulation to speed up the rate of curing at elevated temperatures, which results in the existence of a large amount of ionic substances in the epoxy system. In this study, the addition of TMPTMA monomers with very low and constant ionic contents before and after their curing reactions into epoxy systems diluted the ionic content of the epoxides. In addition, according to AFM and DMA observations, the incorporation of TMPTMA into the epoxy systems resulted in an enhancement in the crosslinking degree of the resulting IPNs; this produced much lower tan δ values in the extra-low-frequency range for the cured CER–anhydride/TMPTMA systems.

These considerations were also supported by the tan δ behaviors of the different epoxy systems in the high-frequency range above 100 Hz [Figs. 7 and 8(b)], where the tan δ value was observed to be apparently higher in the resulting IPNs than in the neat epoxy, and as the concentrations of TMPTMA in the systems increased, the tan δ values of the resulting IPNs gradually increased. This was because the denser crosslinking network of the resulting IPNs in comparison with the neat epoxy resulted in the formation of the more intensive dipole-orientational polarization caused by many more electric dipoles.

The temperature dependences of tan δ also showed an evident difference between the cured

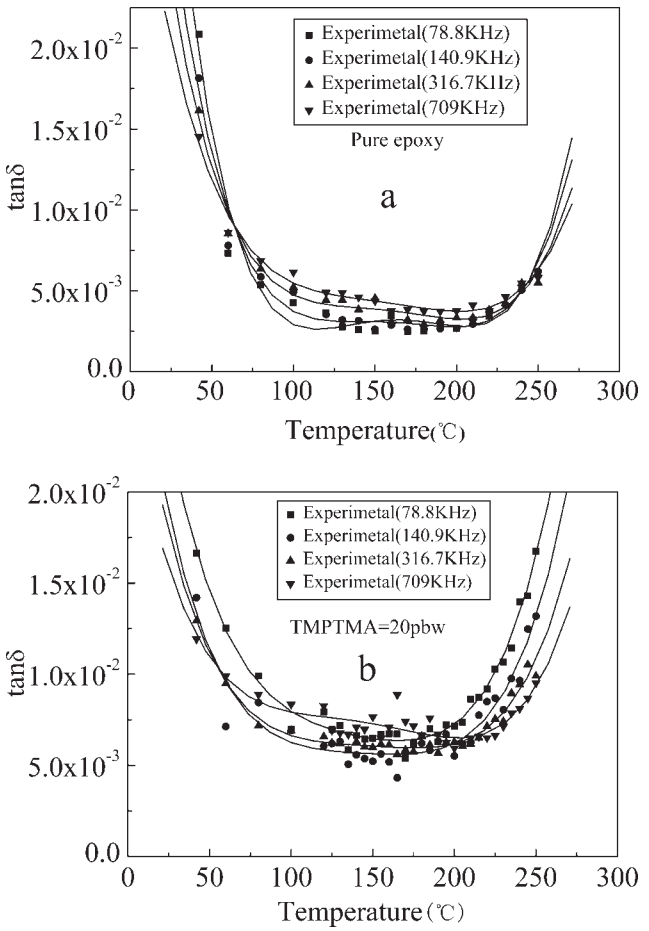


**Figure 9** Temperature dependence of tan δ for epoxides (a) without TMPTMA and (b) with a TMPTMA concentration of 20 pbw.

epoxides with and without the TMPTMA modifier. Figure 9 illustrates the temperature dependences of tan δ for the epoxides without TMPTMA [Fig. 9(a)] and with a TMPTMA concentration of 20 pbw [Fig. 9(b)] at different frequencies. Interestingly, (1) the tan δ value was greater in the pure epoxy than in the resulting IPNs with a TMPTMA concentration of 20 pbw in the comparatively low-temperature range below 50°C, and (2) in the relatively high temperatures over 50°C, the tan δ value tended to be greater in the resulting IPNs with a TMPTMA concentration of 20 pbw in comparison with the pure epoxy.

Because the lower the temperature is, the lower the conductive current flowing through a dielectric is,[23] the tan δ behaviors in the relatively low-temperature range were attributed mainly to the dipole relaxation polarization. As mentioned previously, the pure epoxy had a less dense and relatively simple structure in the crosslinking network compared to the resulting IPNs. The lower the crosslinking degree in a pure epoxy is, the easier the motion of electric dipoles toward the external electric field may become, which causes an increase in the dielectric loss pertinent to the dipole relaxation phenomenon, which might be a probable reason why the pure epoxy had higher tan δ values compared to the resulting IPNs at relatively low temperatures.

As shown in Figure 9(b), in the high-temperature range over 200°C, the tan δ behavior of the resulting IPNs was distinguished from that of the pure epoxy. It is well known that at very high temperatures above a critical value, the motion of dipoles toward the direction of the external electric field becomes more and more difficult, whereas both the amount of the free charge carriers and the ionic mobility tend to increase significantly. Also, the resulting IPNs are higher in molecular density than the pure epoxy, which led to the expectation that at the aforementioned high temperatures, the former may have contained the more conductive elements, including free and/or semifree conductive ions caused by thermal decomposition of the curing network.

Therefore, at high temperatures over the vitrification temperature, the dielectric loss due to the electrical conduction was likely to be predominant over that due to the dipole relaxation, which can be expressed as

$$\tan\delta = \frac{A}{\omega\varepsilon_0\varepsilon_\infty}\exp\left(\frac{-B}{T}\right) \quad (4)$$

where $A$ and $B$ are constants.[23]

Also, the temperature dependence of the tan δ value in the high-temperature range over 200°C had apparent frequency-dependent characteristics; that is, the higher the frequency was, the further the tan δ value at an arbitrary temperature was lowered.

The measurement results for direct-current resistivity provide the useful data for explaining the aforementioned dielectric behaviors of the cured epoxides. Table II gives a comparison of direct-current resistivity for the epoxides with and without TMPTMA. The value of the direct-current resistivity of the resulting IPNs was larger than that of the pure epoxy at low temperatures, whereas the opposite result was observed in the high-temperature range, which showed that the dielectric behaviors of the resulting IPNs at comparatively low temperatures may have been related to their structural

**TABLE II**
**Comparison of the Direct-Current Resistivity Values for Cured Epoxides with and Without TMPTMA**

| Sample | Direct-current resistivity (Ω m) | |
|---|---|---|
| | 50°C | 210°C |
| With no TMPTMA | $3.66 \times 10^{13}$ | $5.50 \times 10^{12}$ |
| With 20 pbw TMPTMA | $6.79 \times 10^{13}$ | $1.98 \times 10^{12}$ |

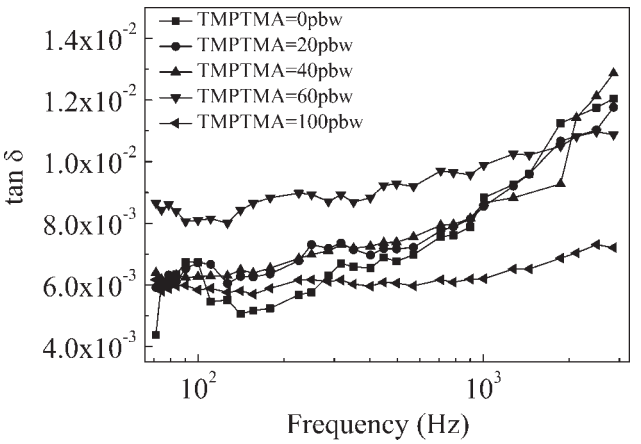


**Figure 10** Frequency dependence of tan δ for epoxides with different concentrations of TMPTMA.

characteristics as distinguished from the crosslinking network of the conventional pure epoxides and that the high-temperature characteristics of the dielectric behavior could be explained by means of the conductive loss mechanism.

The temperature in which tan δ began to sharply increase (Fig. 9) was nearly in accordance with the glass-transition temperatures of the CER/TMPTMA systems observed in DMA measurements.[16]

Also, as clearly shown in Figure 10, the tan δ for the epoxides without any modifiers or with a relatively low concentration of TMPTMA below 40 pbw tended to increase significantly with increasing frequency, whereas with high contents of TMPTMA above 40 pbw, tan δ showed little change in a comparatively wide range of frequency (70 kHz–3 MHz).

In the aforementioned frequency range, the increase in tan δ with increasing frequency meant that the main mechanism of dielectric loss could be attributed to dipole relaxation polarization because the conduction loss due to the ionic motion could be neglected at room temperature and/or at such relatively high frequencies and is known to become lower and lower with increasing frequency.

From the fact that tan δ of the resulting IPNs with comparatively high contents of TMPTMA above 40 pbw showed less significant changes in the frequency range 70 kHz–3 MHz, we concluded that the chemical and physical interactions between dipoles were so intense at room temperature because of the dense crosslinking networks that the frequency of the external electric field applied to the specimen had little influence on the motion of dipoles. However, the orientation of dipoles in the pure epoxy or in the resulting IPNs with relatively low TMPTMA concentrations below 40 pbw was relatively easy because the crosslinking networks were not as dense as the resulting IPNs with higher TMPTMA concentrations. Therefore, the higher the frequency of the applied electric field was, the more frequent the motion of dipoles was, which resulted in the increase in tan δ with increasing frequency.

### Dielectric permittivity measurement

Figure 11 gives the frequency dependences of the permittivities of the epoxides with different concentrations of TMPTMA. In the resulting IPNs investigated in this study, the dielectric permittivity tended to decrease with increasing TMPTMA concentration. This phenomena can be explained by the fact that the denser the crosslinking network was, the more difficult the orientation of dipoles toward the external electric field was because of the more intensive interactions between the neighboring dipoles.

Of great interest is that, in the whole frequency range, the frequency dependences of the dielectric parameters showed analogous change behaviors both in the neat cured epoxide and in the IPNs, which suggested that no phase separation existed between the two individual crosslinking networks forming the aforementioned sIPNs, which was in good agreement with DMA results (Fig. 4).

### Alternating-current resistivity measurement

As illustrated in Figure 12, the frequency dependence of the alternating-current resistivity was also quite similar in its change behaviors to that of tan δ. In the low-frequency range below 10 Hz, the alternating-current resistivity of the neat epoxy was distinctly lower than those of the resulting IPNs [Fig. 12(a)], whereas a contrary tendency in the alternating-current resistivity values between the resulting IPNs and the neat epoxy was observed in the high-frequency range above 10 Hz [Fig. 12(b,c)]. The

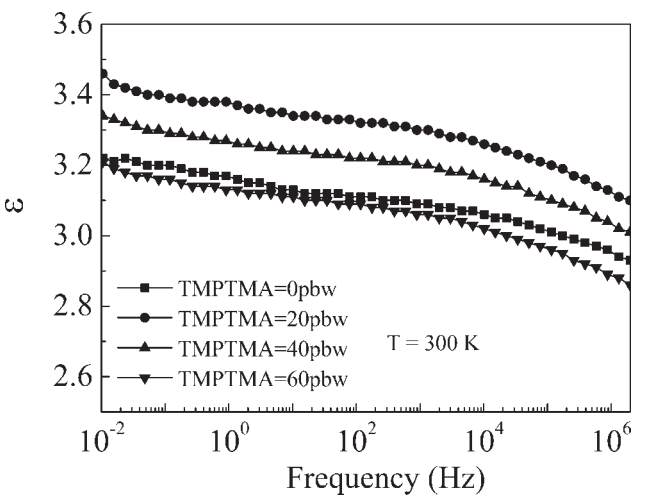


**Figure 11** Frequency dependence of the dielectric permittivity (ε) of epoxides with different concentrations of TMPTMA.

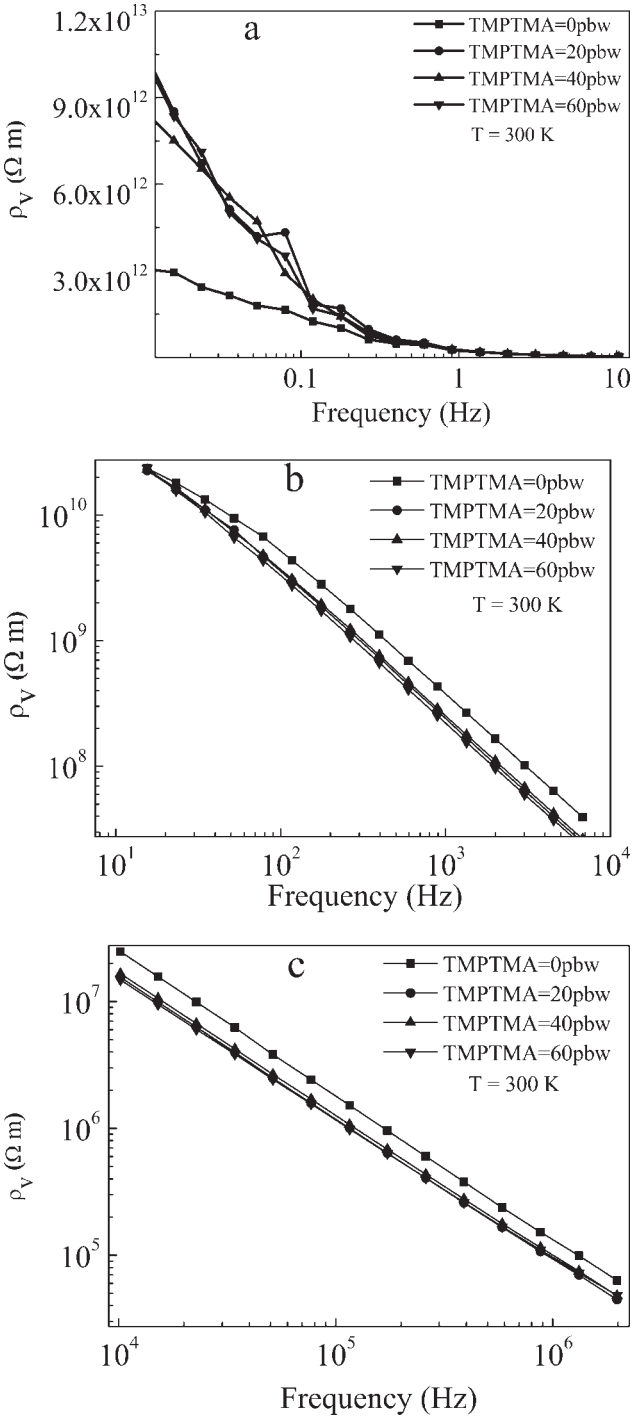


**Figure 12** Frequency dependence of the alternating-current resistivity ($\rho_v$) for cured epoxides with different concentrations of TMPTMA in (a) the extra-low frequency range, (b) the middle frequency range, and (c) the high frequency range.

concentration of TMPTMA has no apparent influence on the alternating-current resistivity values of the resulting IPNs in the frequency range from $10^{-2}$ to $10^6$ Hz. These phenomena may be attributed to the crosslinking structures of the cured epoxides with and without the modifier TMPTMA and the species and numbers of free carriers in these cured epoxides systems.

## CONCLUSIONS

As a result of the incorporation of the TMPTMA network into the CER–anhydride network, uniform and compact microstructures in the cured CER/TMPTMA systems were obtained during the curing procedures. The existence of the higher crosslinking density in the resulting IPNs was proven by DMA measurement and AFM observations.

The thermal and dielectric performances of the resulting IPNs were strongly dependent on their microstructures. The TGA and DTA results imply that there was an enhancement in the thermal stability to some extent, and the dielectric investigations showed that the resulting IPNs displayed dielectric behaviors different from those of the neat epoxy:

1. The tan δ value in the extra-low-frequency range was much higher in the neat epoxy than in the resulting IPNs, and in the high frequency range above 100 Hz, the tan δ value was apparently higher in the resulting IPNs than in the neat epoxy.
2. The temperature dependences of tan δ for the resulting IPNs also showed an evident difference between the dielectric behaviors of the cured epoxides with and without the modifier TMPTMA.
3. The dielectric permittivity of resulting IPNs tended to decrease in the frequency range 0.01 Hz–1 MHz with increasing TMPTMA concentration.
4. The changes in the alternating-current resistivity values of the cured epoxides without and with TMPTMA were quite apparent in the frequency range $10^{-2}$–$10^6$ Hz, but the concentration of TMPTMA had no effect on the alternating-current resistivity value in the cured epoxides.

### References

1. Edward, A. B.; Stone, G. C. IEEE Electr Insul Mag 2004, 20, 25.
2. Weege, T. Proc Electr/Electron Insul Conf, Sept 22–25, 1997, 709.
3. Fazio, C. Proc Electr/Electron Insul Conf, Sept 22–25, 1997, 753.
4. Lee, K. Y.; Lee, K. W.; Choi, Y. S.; Park, D. H. IEEE Trans Dielectr Electr Insul 2005, 12, 566.
5. Joseph, R. N.; Balaji, N. Polymer 2006, 47, 1108.
6. Boey, F.; Lath, S. K.; Ng, A. K.; Abadie, M. J. M. J Appl Polym Sci 2002, 86, 518.
7. Teil, H.; Page, S. A.; Michaud, V.; Manson, J. A. E. J Appl Polym Sci 2004, 93, 1774.
8. Zhuqing, Z.; Wong, C. P. J Appl Polym Sci 2002, 86, 1572.
9. Smith, J. D. B. J Appl Polym Sci 1981, 26, 979.

10. Dean, K.; Cook, W. D.; Burchill, P.; Zipper, M. Polymer 2001, 42, 3589.
11. Montserrat, S.; Andreu, G.; Cortes, P.; Calventus, Y.; Colomer, P.; Huntchinson, J. M.; Malek, J. J Appl Polym Sci 1996, 61, 1663.
12. Cortes, P.; Montserrat, S.; Huntchinson, J. M. J Appl Polym Sci 1997, 63, 17.
13. Nunez-Regueira, L.; Villanueva, M.; Fraga-Rivas, I. J Therm Anal Calorim 2006, 86, 463.
14. Ali, M.; Hammami, A. Polym Compos 2005, 26, 593.
15. Joseph, R. N.; Balaji, N. Polymer 2006, 47, 1108.
16. Duan, J.; Kim, C.; Jiang, P. J Polym Res, to appear.
17. Park, S.-J.; Kwak, G.-H.; Sumita, M.; Lee, J.-R. Polym Eng Sci 2000, 40, 2569.
18. Galy, J.; Sabra, A.; Pascault, J.-P. Polym Eng Sci 1986, 26, 1514.
19. Lee, D. G.; Kim, H. G. J Compos Mater 2004, 12, 977.
20. Liming, Z.; Leo, C. K.; Martin, C. H. Polymer 2005, 46, 2638.
21. Yangyang, S.; Zhuqing, Z.; Wang, C. P. Polymer 2005, 46, 2297.
22. Guo, Z.; Warner, J.; Christy, P.; Kranbuehl, D. E.; Boiteux, G.; Seytre, G. Polymer 2004, 45, 8825.
23. Smith, J. D. B.; Kauffman, R. N. IEEE Trans Electr Insul 1984, 19, 33.
24. Dusek, K.; Matejka, L.; Spacek, P.; Winter, H. Polymer 1996, 37, 2233.
25. Qin, C.-L.; Cai, W.-M.; Cai, J.; Tang, D.-Y.; Zhang, J.-S.; Qin, M. Mater Chem Phys 2004, 85, 402.
26. Dean, K. M.; Cook, W. D.; Lin, M. Y. Eur Polym J 2006, 42, 2872.
27. Tobolsky, A. V. Properties and Structure of Polymers; Wiley: New York, 1960.
28. Kremer, F.; Schonhals, A. Broadband Dielectric Spectroscopy; Springer-Verlag: Berlin, 2002.